

Supporting Information

Ultrafast kinetics in a phase separating electrode material by forming an intermediate phase without reducing the particle size

Minkyung Kim^{†‡}, Mihee Jeong[§], Won-Sub Yoon[§], Byoungwoo Kang^{†*}

[†]Department of Materials Science and Engineering, Pohang University of Science and Technology (POSTECH), Pohang 37673, Republic of Korea

[‡] Energy Storage and Distributed Resources Division, Lawrence Berkeley National Laboratory, Berkeley, California 94720, United States

[§]Department of Energy Science, Sungkyunkwan University, Suwon, 440-746, Republic of Korea

Table S1. Lattice parameters of PTFE-LiVPO₄F and CTR-LiVPO₄F by Rietveld refinement

PTFE-LiVPO ₄ F						
P $\bar{1}$: Z=2 a = 5.1835(4) Å, b = 5.3124(2) Å, c = 7.2672(2) Å alpha = 107.582(3)°, beta = 107.955(2)°, gamma = 98.447(7)° Volume = 175.007(8) Å ³						Bragg R-factor: 6.62 RF-factor : 5.17
Atomic Parameters						
Atoms	Wyckoff position	x/a	y/b	z/c	Occ.	B _{iso}
V(1)	1a	0	0	0	1	0.404
V(2)	1b	0	0	0.5	1	0.306
P	2i	0.31889(90)	0.64652(87)	0.24986(83)	1	0.557
O(1)	2i	0.36980(177)	0.24044(148)	0.58599(137)	1	0.842
O(2)	2i	0.11048(186)	-0.32998(146)	0.36133(139)	1	0.299
O(3)	2i	0.68291(180)	0.66372(180)	-0.13847(125)	1	0.752
O(4)	2i	0.27067(157)	0.79328(152)	0.08892(129)	1	0.425
F	2i	-0.11871(137)	0.64652(87)	0.24535(117)	1	0.417
Li	2i	0.70771(656)	0.38817(593)	0.22343(476)	1	2.635
CTR-LiVPO ₄ F						
P $\bar{1}$: Z=2 a = 5.1752(6) Å, b = 5.3086(7) Å, c = 7.2653(5) Å alpha = 107.571(1)°, beta = 107.980(8)°, gamma = 98.354(4)° Volume = 174.627(7) Å ³						Bragg R-factor: 7.33 RF-factor : 5.99
Atomic Parameters						
Atoms	Wyckoff position	x/a	y/b	z/c	Occ.	B _{iso}
V(1)	1a	0	0	0	1	0.404
V(2)	1b	0	0	0.5	1	0.306
P	2i	0.31839(92)	0.64696(94)	0.25105(83)	1	0.557
O(1)	2i	0.36980(177)	0.24044(148)	0.58599(137)	1	0.842
O(2)	2i	0.11048(186)	-0.32998(146)	0.36133(139)	1	0.299
O(3)	2i	0.68980(190)	0.66587(193)	-0.13714(134)	1	0.752
O(4)	2i	0.27660(167)	0.78845(164)	0.08893(139)	1	0.425
F	2i	-0.11544(149)	0.09029(149)	0.24906(124)	1	0.417
Li	2i	0.70426(693)	0.39044(631)	0.20041(469)	1	2.635

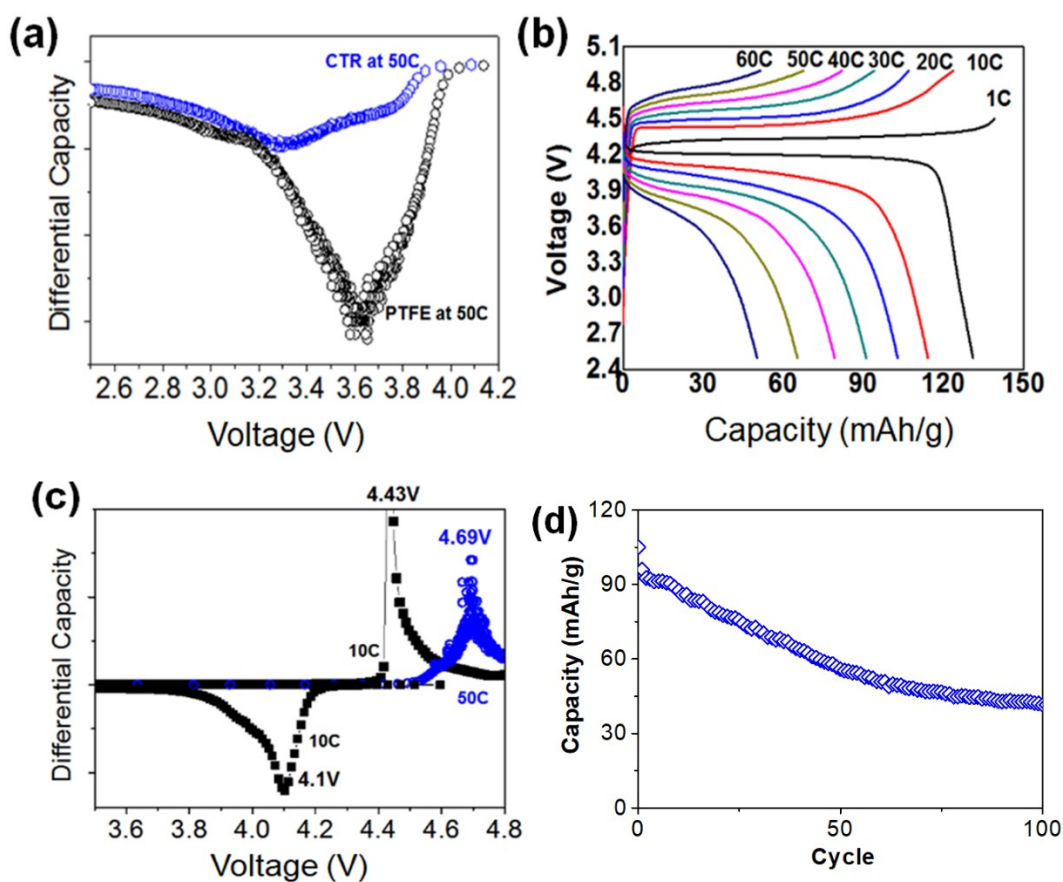


Figure S1. (a) Differential capacity plot of PTFE-LiVPO₄F and CTR-LiVPO₄F of **Figure 2a** and **2b** (a 50C discharge rate). Voltage polarization is much higher in CTR-LiVPO₄F sample than the PTFE-LiVPO₄F. (b) Voltage profiles of **Figure 2e** of PTFE-LiVPO₄F (c) Differential capacity plot (dQ/dV) of (b) at a 10C and 50C charge rate. (d) Cycle retention of CTR-LiVPO₄F. It was charged and discharged at 1C rate (4.5-3V).

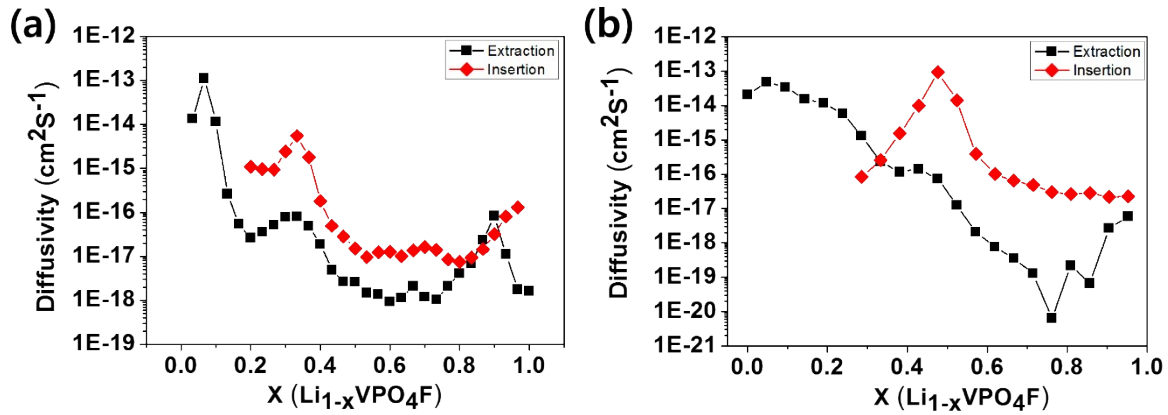


Figure S2. Calculated Li ion diffusivity from galvanostatic intermittent titration technique (GITT) method of (a) PTFE-LiVPO₄F and (b) CTR-LiVPO₄F.

This calculation was based on the below equation (1) developed by Weppner et. al.

$$D_{Li^+} = \frac{4}{\pi} \left(\frac{V_M}{SF} \right)^2 \left(I_0 \frac{\delta E_s / \delta x}{\delta E / \delta t^{1/2}} \right)^2 \text{ at } t \ll \tau \text{ ----- (1)}$$

where V_M is molar volume $5.2346 \times 10^{-5} \text{ m}^3/\text{mol}$, S is the electrode surface area of each samples, F is the Faraday's constant $96,485.3365 \text{ C/mol}$, I_0 is the pulse current, $\delta E_s / \delta x$ is the slope of equilibrium open circuit voltage (OCV) with respect to Li amount, which can be obtained from the differential of OCV curve, and $\delta E / \delta t^{1/2}$ is the slope of initial transient voltage change with respect to square root of time.

The diffusivities are changed depending on the lithium composition in both samples, PTFE-LiVPO₄F and CTR-LiVPO₄F. In both LiVPO₄F samples, carbon was included with LiVPO₄F, so the surface area of the composite sample (LiVPO₄F + carbon) was considered. The measured Li diffusivity of PTFE-LiVPO₄F was compared with the reported Li diffusivity of LiVPO₄F by P.F. Xiao et. al.¹ The range of the two diffusivities are similar to each other.

Table S2. Electronic conductivities of the composite samples that have LiVPO₄F and carbon. Each sample was pelletized, and then Ag paste was put on the top and bottom of the pellets. Direct current (DC) measurement was conducted to the pellets with stainless collector.

PTFE-LiVPO₄F	CTR-LiVPO₄F
9.0 x 10⁻³ S/cm	6.4 x 10⁻³ S/cm

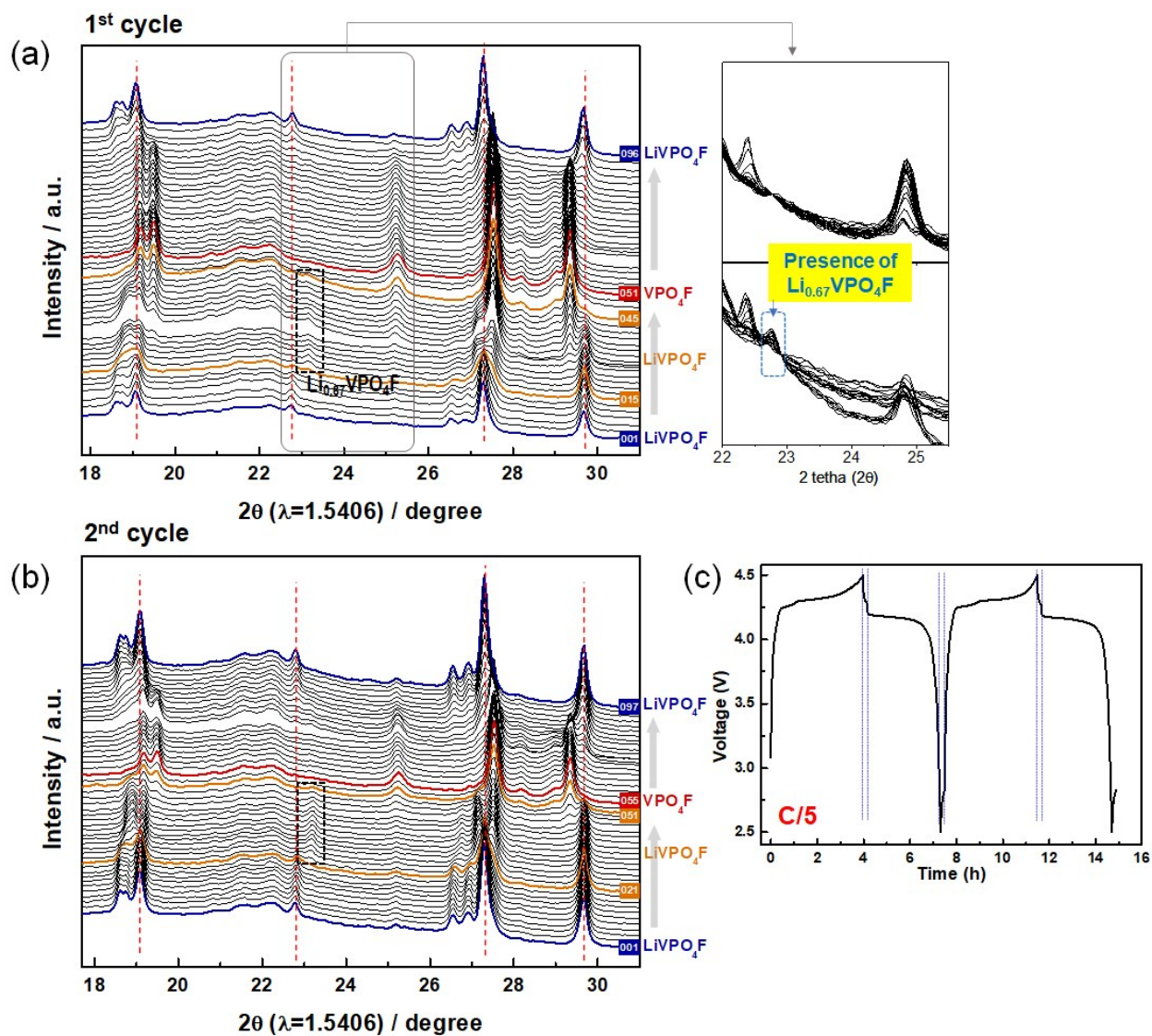


Figure S3. Operando synchrotron XRD patterns of CTR-LiVPO₄F for 2 cycles. XRD diffraction patterns represent at (b) 1st cycle and (c) 2nd cycle. Red dash vertical lines indicate main peaks of LiVPO₄F. (c) its voltage profile for 2 cycles. It was charged at C/5 rate and discharged at C/5 rate. The cell was rested for 10 mins after each step during charge/discharge (blue dash vertical lines)

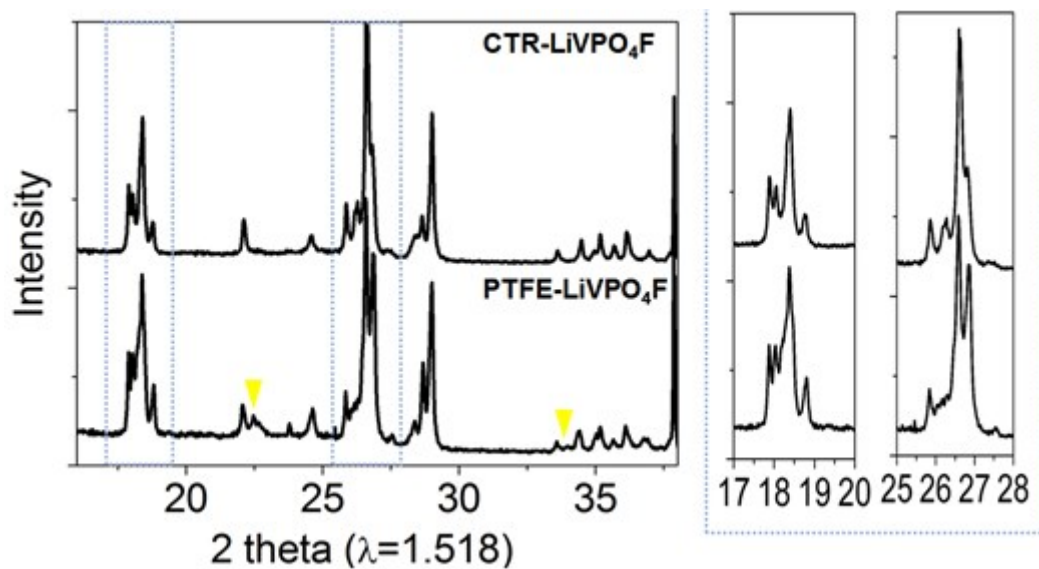


Figure S4. High resolution powder synchrotron XRD patterns of *ex situ* electrodes of CTR-LiVPO₄F and PTFE-LiVPO₄F at DOD50 (Depth of Discharge 50%), which is a Li_{0.5}VPO₄F with the lithiation, at a C/5 rate.(▼: Li_{0.67}VPO₄F). Main peak shapes were different due to the introduction of the intermediate phase.

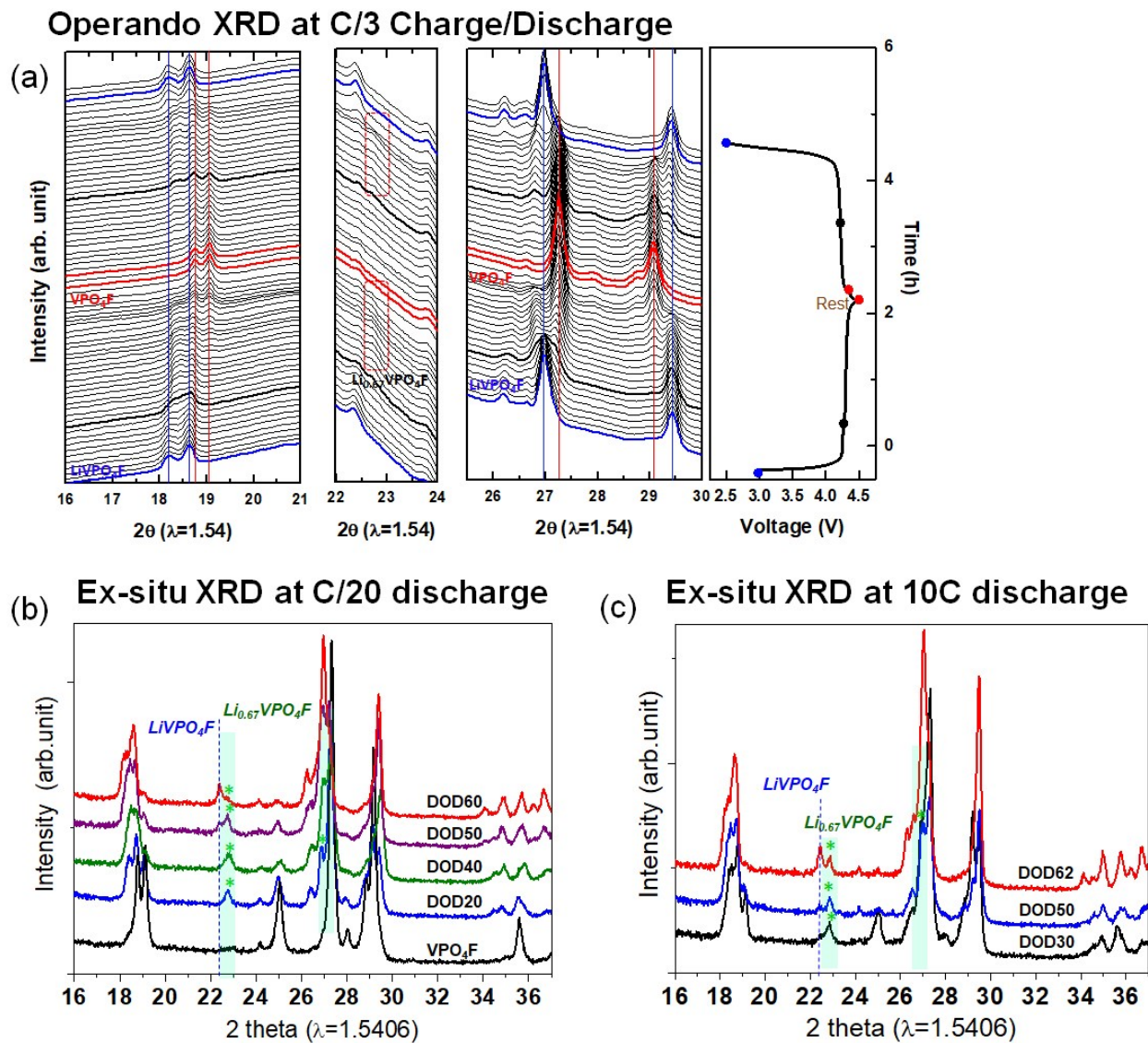


Figure S5. Phase transformation behaviors in PTFE- LiVPO_4F at various C-rates (a) Operando synchrotron XRD patterns at C/3 charge rate and C/3 discharge rate and its voltage profile. *Ex situ* XRD patterns at (b) C/20 discharge rate and (c) 10C discharge rate. Both cells were charged at C/5 rate. Depth of Discharge (DOD) was described on each XRD pattern.

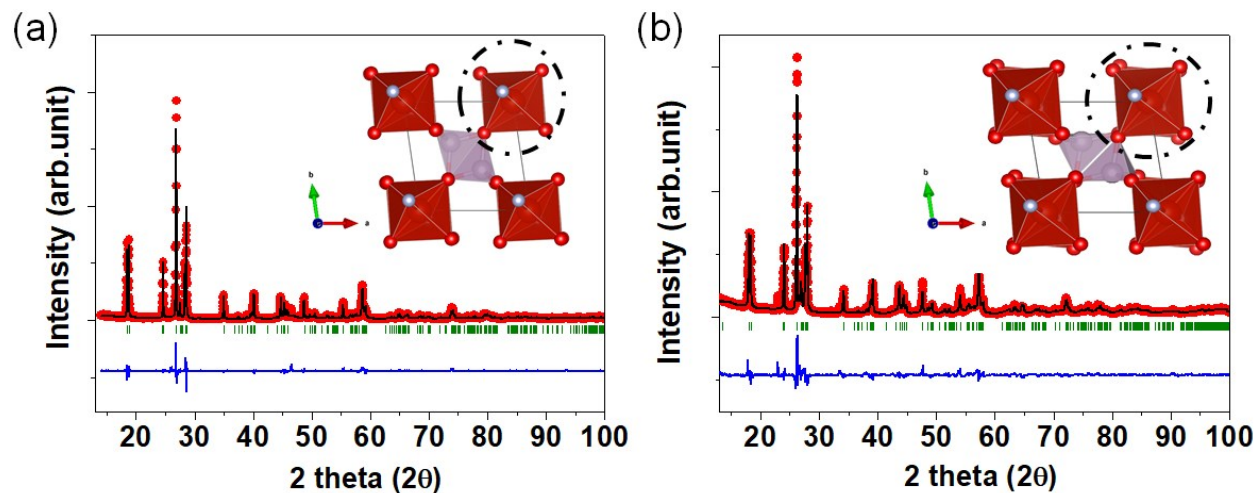


Figure S6. Synchrotron XRD patterns of chemically delithiated (a) CTR-VPO₄F and (b) PTFE-VPO₄F. Monoclinic VPO₄F structure is converted to triclinic with assuming VPO₄F forms by fully extracting Li ions from triclinic LiVPO₄F. Rietveld refinement was conducted using triclinic VPO₄F. More details are our previous study.² Based on the calculation, the dihedral angle of VO₄F₂ octahedra in VPO₄F can be an indicator for the amount of the oxygen defects in the materials. The dihedral angle of VO₄F₂ octahedra in VPO₄F is ~ 2.2° and ~ 4° for experimentally synthesized CTR-VPO₄F and PTFE-VPO₄F, respectively. This indicates that PTFE-LiVPO₄F can have less amount of the oxygen defects than CTR-LiVPO₄F

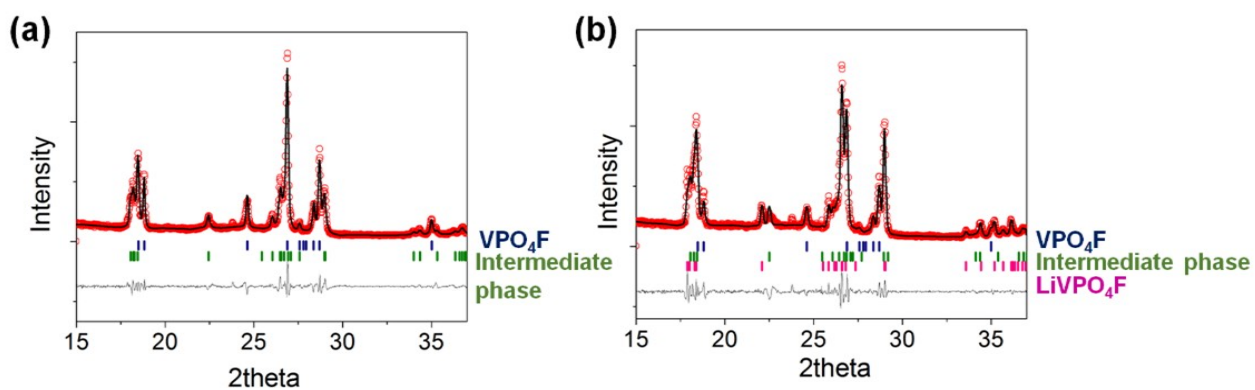
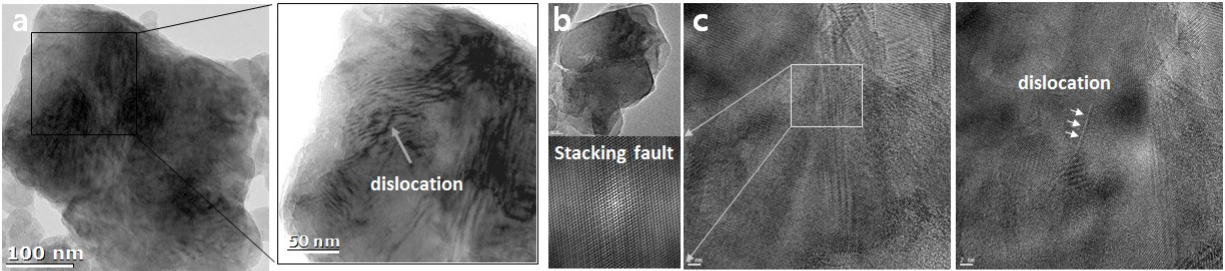


Figure S7. Synchrotron XRD patterns of *ex situ* electrodes of PTFE-LiVPO₄F at (a) DOD20, which is a Li_{0.2}VPO₄F with the lithiation of 20 % Li, and (b) DOD50, which is a Li_{0.5}VPO₄F with the lithiation of 50 % Li. These XRD patterns were analyzed by a profile matching. Red dots represent an observed data, black lines represents the theoretical Bragg patterns of the phases. Gray line is the difference between the observed pattern and the theoretical one. (R-factor: 5.89, Chi²: 4.04 in (a), R-factor: 5.53, Chi²: 4.57 in (b))

CTR



PTFE

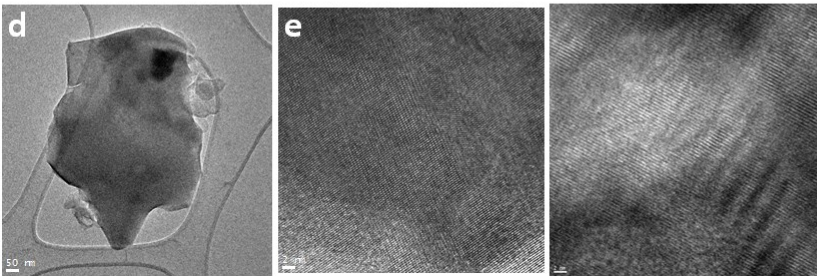


Figure S8. TEM measurements of particles in electrochemically lithiated two samples with DOD50. Structural analyses of the CTR- $\text{Li}_{0.5}\text{VPO}_4\text{F}$ (a) Low magnification image with its enlarged image of the dislocation part, (b) Low magnification image and (c) its high resolution image of stacking faults and dislocations. Structural analyses of the PTFE- $\text{Li}_{0.5}\text{VPO}_4\text{F}$ (d) Low magnification image and (e) its high resolution image. Much more structural defects such as stacking faults and dislocations are observed in the CTR- LiVPO_4F than the PTFE- LiVPO_4F .

Reference

1. P. F. Xiao, M. O. Lai and L. Lu, *Solid State Ionics*, 2013, **242**, 10-19.
2. H. Park, M. Kim, S. Kang and B. Kang, *Journal of Materials Chemistry A*, 2019, **7**, 13060-13070.